



	<b>Experiment title:</b> "Chemical and structural modifications in cerium oxide nanoparticles of selected size during controlled reduction/oxidation"	<b>Experiment number:</b> HC 2724
<b>Beamline:</b> ID 26	<b>Date of experiment:</b> From: 09/11/2016 To: 16/11/2016	<b>Date of report:</b>  <i>Received at ESRF:</i>
<b>Shifts:</b> 15	<b>Local Contact:</b> Alessandro Puri	

**Names and affiliations of applicants (\* indicates experimentalists):**

Paola Luches<sup>1</sup>, Jacopo Stefano Pelli Cresi\*<sup>2</sup>, Maria Chiara Spadaro\*<sup>2</sup>, Sergio D'Addato<sup>2</sup>, Federico Boscherini\*<sup>3,4</sup>

<sup>1</sup> Centro S3, Istituto Nanoscienze, Consiglio Nazionale delle Ricerche, Modena, Italy

<sup>2</sup> Department of Physical, Information and Mathematical Sciences, University of Modena and Reggio Emilia, Modena, Italy

<sup>3</sup> Dipartimento di Fisica e Astronomia, Università di Bologna, Viale C. Berti Pichat 6/2, 40127 Bologna, Italy

<sup>4</sup> Operative Group in Grenoble, Istituto Officina dei Materiali, Consiglio Nazionale delle Ricerche, c/o ESRF, BP 220, F-38043, Grenoble, France

**Report:**

In this experiment we followed in-situ the structural and electronic modification of cerium-oxide nanoparticles (NP) of different size during reducing thermal treatments. This goal was achieved by acquiring EXAFS and XANES measurements at the Ce L<sub>3</sub> edge, which are very sensitive to small structural modifications and to the cerium ion oxidation state.

According to some previous studies, cerium oxide NP show higher reducibility than (111) oriented ultrathin films with comparable surface to volume ratio [1]; this may be due to dimensional effects and/or to the presence of surface terminations less stable than the (111). The goal of this experiment was to understand the role of dimensionality in the modification of the oxide properties.

The CeO<sub>2</sub> NPs samples were grown by magnetron sputtering and inert gas aggregation in mixture of Ar and He gases. The NP were selected in mass with a quadrupole filter and deposited on a Si/SiO<sub>x</sub> substrate. The size of the obtained NP was checked by TEM after the growth. In the present experiment we investigated films with different NP diameter: 3 nm and 4.5 nm. Two 3 nm diameter NP films with different nominal thickness - 5 nm and 10 nm - were prepared, the thicker one was expected to give a better signal, although it could be affected by more severe aggregation effects induced by the thermal treatment. The samples were prepared in our laboratories and carried to the ESRF in a non reactive atmosphere.

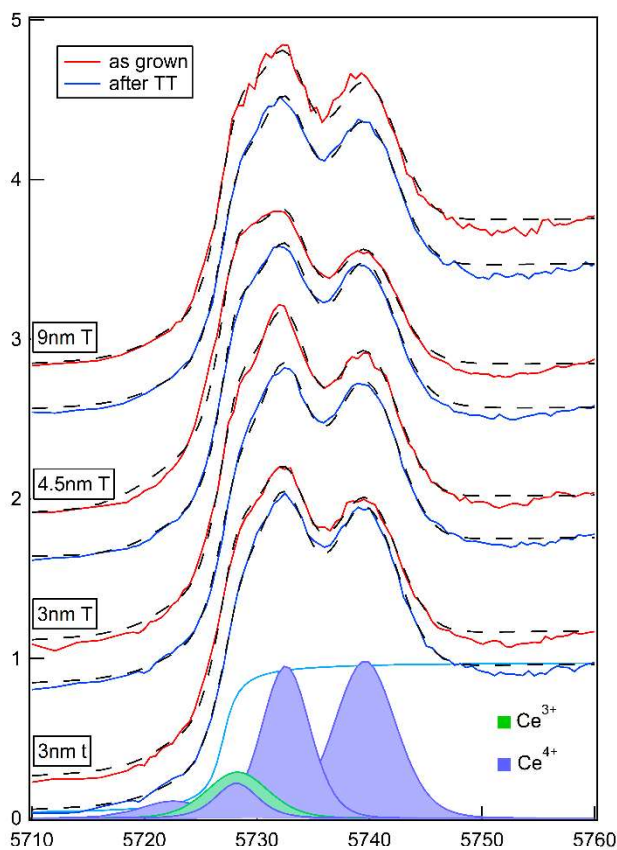
A microtomo furnace was used to perform the reducing thermal treatments in high vacuum (P=10<sup>-7</sup> mbar). We measured each sample before and after thermal treatment at 1025 K for 30 min in high vacuum. The heating and cooling rates, controlled by a PID, were set to 7 K/min for all samples. The Ce L<sub>3</sub>-edge spectra were acquired in the fluorescence yield mode with a 13-element Ge detector. Two reference samples containing only Ce<sup>4+</sup> (CeO<sub>2</sub> powders) and Ce<sup>3+</sup> (cerium (III) nitride powders) were also measured in the transmission mode.

Fig.1 reports the Ce L<sub>3</sub>-edge XANES spectra acquired on the three samples before and after the thermal treatments. The XANES of a fourth film made of NP with 9 nm diameter and with a nominal thickness of 10 nm, prepared and treated in a similar way in a previous beamtime (HC 1848), is also shown for comparison. The figure also reports the fitting obtained with a combination of Pearson curves, with position and widths determined by fitting the reference samples, and an arctangent function for the background. The XANES are dominated by Ce<sup>4+</sup>-related spectral features and a mild increase of Ce<sup>3+</sup> concentration can be detected after the thermal treatment.

Fig.2 shows the imaginary part of the Fourier transform of the EXAFS signal in a  $k=2.5-7.5 \text{ \AA}^{-1}$  range for the three NP samples before and after the thermal treatment, compared with the  $\text{CeO}_2$  reference. A contraction of the first shell Ce-O distance in the NP with respect to the bulk value is clearly visible. The thermal treatment induces a relaxation of the Ce-O distance. We ascribe the observed contraction to dimensionality-induced effects, as predicted by previous theoretical work [2]. A first shell data analysis confirms the qualitative observations and gives the Ce-O distances reported in Fig.3.

[1] M. C. Spadaro, et al. "Morphology, structural properties and reducibility of size-selected  $\text{CeO}_2-x$  nanoparticle films." Beilstein Journ. Nanotechnol. 6, 60 (2015).

[2] C. Loschen, et al. "Understanding ceria nanoparticles from first-principles calculations." J.Phys. Chem. C 111 10142 (2007).



**Fig. 1** Ce  $L_3$ -edge XANES of NP with different size and thickness ( $T=10 \text{ nm}$ ,  $t=5 \text{ nm}$ ). Dashed lines are the best fit of the spectra obtained using the  $\text{Ce}^{3+}$  and  $\text{Ce}^{4+}$  components shown at the bottom.

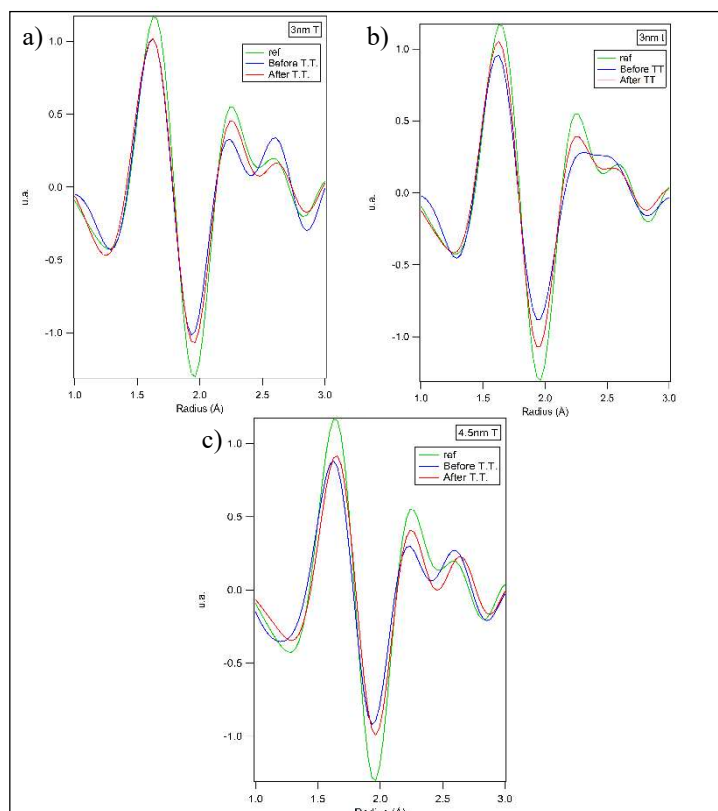


**Fig. 2** Imaginary part of the Fourier transform of the EXAFS signal in the  $k=2.5, 7.5 \text{ \AA}^{-1}$  range for the NP of different size and thickness ( $T=10 \text{ nm}$ ,  $t=5 \text{ nm}$ ), before and after the thermal treatments, in comparison with the  $\text{CeO}_2$  reference sample.

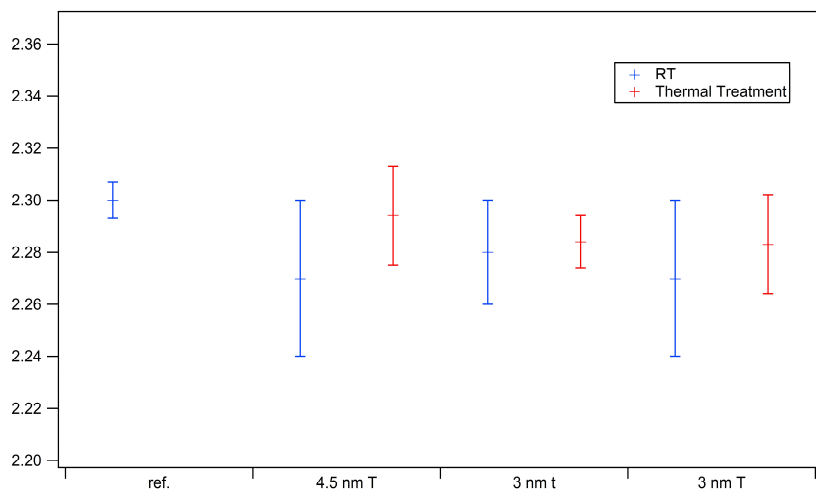


**Fig. 3** First shell Ce-O distances evaluated from the fitting of the EXAFS spectra of the NP of different size before and after the thermal treatments, in comparison with the  $\text{CeO}_2$  reference sample.